

Multiple Diffraction of X-Rays

Roberto Colella

Department of Physics, Purdue University, West Lafayette, Indiana 47907 U.S.A.

Z. Naturforsch. **37a**, 437–447 (1982); received January 22, 1982

Dedicated to Professor Dr. G. Hildebrandt on the occasion of his 60th birthday

The phenomenon of n -beam diffraction ($n > 2$) is discussed with particular attention being devoted to the Bragg case of diffraction. The general method of solution is outlined, and some applications to specific situations are discussed. These include experiments in which strong quasi-monochromatic phonon beams are excited in a crystal using the Acousto-Electric effect, phase determination using the concept of „Virtual Bragg Scattering”, and high resolution Bragg reflection topographs. In all cases the agreement between theory and experiment has been found excellent.

1. Introduction

Several years ago I had an opportunity of sharing an office at Cornell University with Professor Hildebrandt (we were both associated, at that time, with Professor Batterman's laboratory) and through several conversations we had at that time I became acquainted with the problems of n -beam dynamical theory. As a result of this contact, I developed an interest in n -beam dynamical diffraction, did some of my own research in this area during the ensuing years, and it seems fitting now to dedicate this article to Professor Hildebrandt on the occasion of his sixtieth birthday.

Propagation of x-ray photons in a crystal is entirely analogous to propagation of electron waves, commonly described as “Bloch waves”. It is shown in electron band theory, using Bloch theorem, that the electron wave function in a crystal can always be expressed as a superposition of plane waves:

$$\psi_{\mathbf{k}}(\mathbf{r}) = \sum_j C_j e^{i(\mathbf{k} + \mathbf{G}_j) \cdot \mathbf{r}} \quad (1.1)$$

where \mathbf{k} is the electron wave vector, and \mathbf{G}_j are reciprocal lattice vectors. A convenient way of looking at (1.1) is to consider \mathbf{k} as the wave vector of an electron that has entered the crystal from an outside vacuum region, and subsequently gives rise to an infinite number of plane waves by Bragg reflections. In this sense diffraction theory is the analog of band theory. The diffraction problem is, however, simpler because the geometry is well defined. The incident beam is usually monochromatic and well

collimated, characterized by a wave vector \mathbf{k}_0 , which becomes \mathbf{k} after refraction at the entrance surface of the crystal. The Ewald construction immediately tells us how many plane waves are important in the crystal, which enables us to reduce the number of unknown amplitudes C_j 's in Eq. (1.1) to a small number, typically two, three, sometimes four (in the x-ray case). This is not the case for the general problem of electron band theory, in which all possible values of \mathbf{k} must be taken into account, with the consequence that a large number of C_j 's must be determined.

In the x-ray case an equation similar to (1.1) is used, except that vector waves are used instead of scalar waves:

$$\mathcal{D}(\mathbf{r}) = \sum_j \mathbf{D}_j e^{i(\mathbf{k} + \mathbf{G}_j) \cdot \mathbf{r}}, \quad (1.2)$$

where $\mathbf{D}(\mathbf{r})$ is the displacement vector inside the crystal. The expansion (1.2) for vector waves was proposed long before Eq. (1.1) by Ewald [1], and for this reason the plane waves appearing in Eq. (1.2) are sometimes called “Ewald waves”, in analogy with Bloch waves.

Another important difference between diffraction theory and band theory is that in the former a crystal is assumed to be finite, limited by one or more well-defined surfaces. The beams of physical significance are the incident and the diffracted beams. Therefore boundary conditions are to be specified and satisfied. Basically, two geometries are normally used in diffraction experiments. The Laue geometry (or Laue case) is such that incident and diffracted beams are not associated with the same surface. In most cases the crystal is in the

Reprint requests to Prof. R. Colella, Department of Physics, Purdue University, West Lafayette, Indiana 47907, U.S.A.

0340-4811 / 82 / 0500-0437 \$ 01.30/0. — Please order a reprint rather than making your own copy.



Dieses Werk wurde im Jahr 2013 vom Verlag Zeitschrift für Naturforschung in Zusammenarbeit mit der Max-Planck-Gesellschaft zur Förderung der Wissenschaften e.V. digitalisiert und unter folgender Lizenz veröffentlicht: Creative Commons Namensnennung-Keine Bearbeitung 3.0 Deutschland Lizenz.

Zum 01.01.2015 ist eine Anpassung der Lizenzbedingungen (Entfall der Creative Commons Lizenzbedingung „Keine Bearbeitung“) beabsichtigt, um eine Nachnutzung auch im Rahmen zukünftiger wissenschaftlicher Nutzungsformen zu ermöglichen.

This work has been digitalized and published in 2013 by Verlag Zeitschrift für Naturforschung in cooperation with the Max Planck Society for the Advancement of Science under a Creative Commons Attribution-NoDerivs 3.0 Germany License.

On 01.01.2015 it is planned to change the License Conditions (the removal of the Creative Commons License condition “no derivative works”). This is to allow reuse in the area of future scientific usage.

form of a slab dividing the vacuum space into two separate regions. In the Laue case incident and diffracted beams propagate in different regions.

In the Bragg geometry (or Bragg case) incident and diffracted beams propagate in the same vacuum region. In most cases the crystal is thick enough that no beam emerges from the exit surface, so that the crystal can be considered infinite for any practical purpose.

A lot of attention has been devoted in the past to multi-beam cases in the Laue case. This interest was motivated by the discovery [2] that anomalous transmission of x-rays (the Borrmann effect) was enhanced in some cases when three or four beams are simultaneously excited, that is to say, when three or four reciprocal lattice points lie simultaneously on the Ewald sphere in reciprocal space. Professor Hildebrandt made a complete study of this phenomenon [3], and explained it by examining the detailed form of the electric field intensity between lattice planes in a multi-beam situation.

The work to be described in this article will mostly be concerned with the Bragg case, which had not been considered by previous investigators. The main motivation for this choice was that it seemed desirable to be able to interpret a Renninger plot [4] much in the same way as ordinary two-beam dynamical theory allows one to interpret rocking curves from perfect crystals in any conceivable situation. The real reason behind all this is the fact that in multi-beam diffraction the relative phases between the various structure factors involved are not lost, and therefore the Renninger plot contains phase information.

Another area of diffraction physics in which n -beam dynamical diffraction has application is the field of interactions between x-ray photons and phonons. It is not convenient to use thermal phonons for this purpose, because they are diffuse in frequency and wave vectors. It is preferable instead to increase the phonon population of specific branches and frequencies and study the separate effects of well characterized phonon branches. One convenient technique makes use of acoustoelectric (A.E.) phonon amplification. Since however the frequencies of typical A.E. phonons are of the order of 10^9 Hz, quite often phonon satellites partially overlap with Bragg peaks. It is therefore necessary to use an n -beam dynamical approach for interpreting the experimental results.

Recently, a new mechanism of Bragg scattering has been found to be operational in n -beam experiments. It has been called "Virtual Bragg Scattering", because it involves Bragg reflections that correspond to nodes far removed from the Ewald sphere and do not conserve energy. It has been shown that Virtual Bragg Scattering can be utilized for phase determinations even in the case of mosaic crystals.

Finally, we will show that multiple reflections can be the origin of unexpected features in Bragg reflection topographs, and that a proper theoretical treatment of n -beam diffraction is needed for explaining these features.

2. General Solution of the n -Beam Diffraction Problem

The general solution is obtained in a two-step process. Firstly, a set of linear equations is set up for determining the amplitudes D_G in (1.2). A preferred direction is introduced, corresponding to the normal of the crystal surface, on which the incident beam is impinging. Only the tangential component of \mathbf{k} is determined. The normal component γ_0 will be determined by a determinantal equation. The set of linear equations for D_G are the well known dynamical equations, obtained after insertion in Maxwell equations of the expansion (1.2), with the crystal polarizability also being expanded into a Fourier series. The following equation is obtained:

$$[k_0^2/\beta_i^2 - (1 - \psi_0)]D_i - \sum_{j=1}^n \psi_{i-j}(\mathbf{u}_i \cdot \mathbf{D}_j)\mathbf{u}_i - D_j = 0, \quad (2.1)$$

where $k_0 = 1/\lambda$, $\beta_i = \mathbf{k} + \mathbf{G}_i$, ψ_i is the Fourier component of the polarizability per unit volume (times 4π) associated with the node \mathbf{G}_i , and $\mathbf{u}_i = \beta_i/\beta_i$ [5]. Since all \mathbf{D}_j 's are normal to β_j , only two components of \mathbf{D}_j need to be specified. The total number of unknown amplitudes is therefore $2n$. At this point an important approximation is introduced in standard dynamical theory. The first factor in brackets of (2.1) is written as $(\psi_0 - 2\delta_i)$ where $\delta_i + 1$ is the refractive index for the i -beam. This is possible because k_0 and β_i differ by a few parts in 10^{-5} . Since all δ_i can be related by linear equations, this procedure consists in linearizing the dynamical equations with respect to the variable whose eigenvalues are sought. While this approximation is ordinarily legitimate in absence of beams grazing the surface,

which seldom happens in the two beam cases, it is not permissible anytime one of the excited beams is parallel to the surface, which is not infrequent in n -beam diffraction. Furthermore, the linearization procedure reduces the number of wave fields from $4n$ to $2n$, which gives rise to problems in satisfying the boundary conditions. The determinantal equation generated by Eq. (2.1) gives rise to $4n$ wave fields.

The second step toward a general solution of the n -diffraction problem consists in establishing the boundary conditions on both surfaces simultaneously, for all crystal and vacuum beams. The boundary conditions are written for the tangential components of \mathbf{E} and \mathbf{H} , and for the normal components of \mathbf{D} and \mathbf{B} . Considering the interdependence of some of the equations, a total of four scalar equations is obtained for each beam. The number of equations generated by the boundary conditions ($4n$) therefore is equal to the number of Ewald waves inside the crystal. The strength of each Ewald wave can therefore be determined by solving the boundary conditions. In this way all vacuum amplitudes are evaluated and the intensities of all beams can be calculated. The details of the procedure for determining the $4n$ eigenvalues and for solving the boundary conditions have been described previously [6], and will not be repeated here.

A computer program has been developed for performing all the computations, in which n , the number of beams, can be any value ≥ 2 . It is sometimes advantageous to use this program even in the two beam case, because it can handle correctly the situation of grazing incident or diffracted beams, to which the standard approximations, such as those, for example, used by Zachariasen in his book [7], are not applicable. The program has been tested against experiment in various ways. For example, the intensities of some "Umweganregung" peaks associated with the (222) reflection in germanium have been calculated and found in agreement with the experimental values within 4–5% [6]. In Fig. 1 we show the plot of the Ge-222 integrated intensity (with respect to θ , the angle of incidence), using Cu-K α , as a function of the azimuthal angle φ . Note that the range $\Delta\varphi$, within which three-beam excitation is appreciable, amounts, for the Umweganregung 222–113 peak, to 22.8 seconds. The 222–113 is the strongest peak in the 222 Renninger plot of germanium. In Fig. 2 we show two rocking

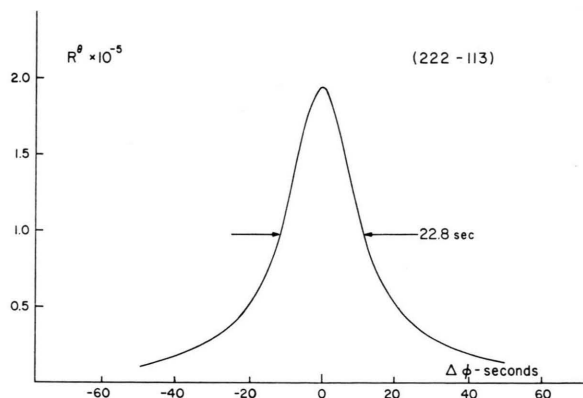


Fig. 1. Calculated integrated intensity of the 222 reflection as a function of the azimuthal angle. Each point of this profile represents an integration of the crystal reflectivity with respect to θ , angle of incidence. The tails tend asymptotically to the "true" 222 value, which is a negligible fraction of the peak value. The abscissa $\Delta\varphi = 0$ corresponds to full excitation of the 113 simultaneous reflection, as obtained from a kinematic calculation.

curves, at different azimuthal angles φ . Note that the peak reflectivity is generally in excess of 50%. Finally in Fig. 3 we show a double crystal rocking curve obtained with both crystals set for simultaneous excitation of the (222) and (113). In this experiment the vertical divergence [8] of the beam between the two crystals is in the range of 20 to 25 seconds of arc. The agreement between theory and experiment is excellent except in correspondence of the maximum peak. It was found later that the crystals used in this experiment were not really perfect, which may explain the lack of agreement in the peak region.

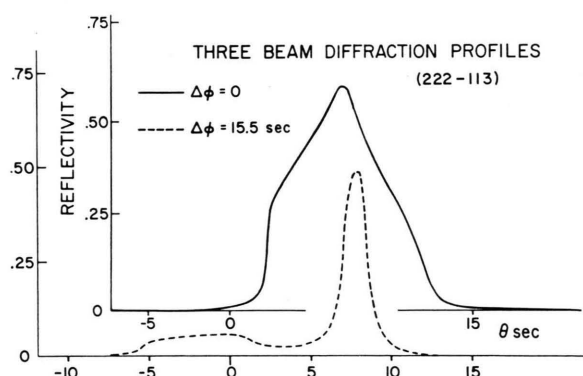


Fig. 2. Computed profiles of three-beam reflectivities vs angle of incidence, for two different values of the azimuthal angle. $\Delta\varphi = 0$ corresponds to full excitation of the 113 simultaneous reflection. The abscissa $\theta = 0$ corresponds to the Bragg angle, without refraction correction, for the "true" 222.

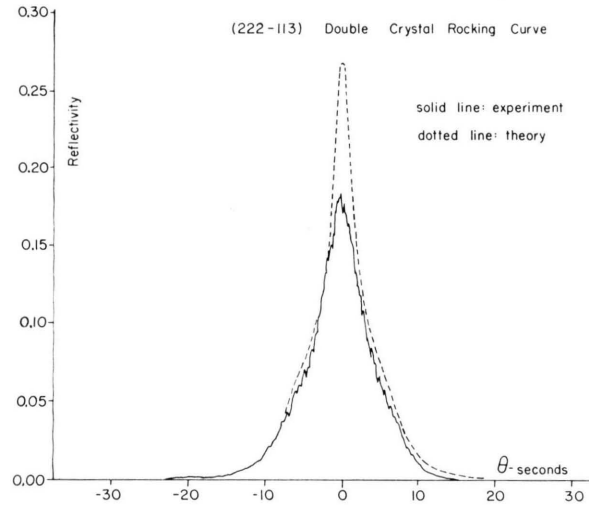


Fig. 3. Double-crystal rocking curve of the 222-113 three-beam reflection, using the anti-parallel arrangement. Both crystals are set for the 222, their azimuths being adjusted for simultaneous excitation of the 113.

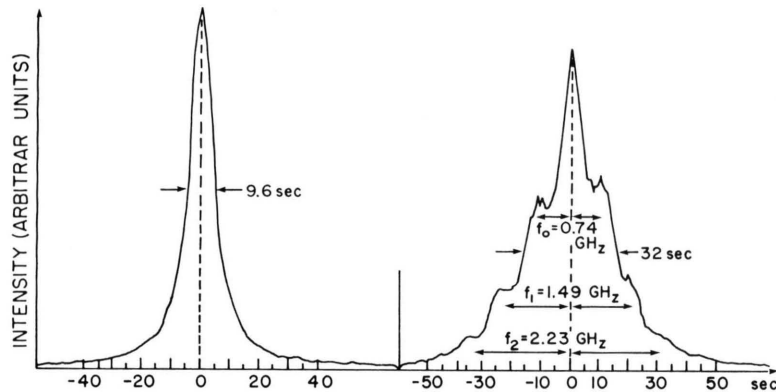


Fig. 4. Double-crystal 004 rocking curve of InSb single crystal, in presence (right-hand side) and absence (left-hand side) of acousto-electric phonons, at 77 °K. Note the presence of second and, perhaps, third order satellites. Peak x-ray intensity was 2000 counts/sec. Carrier concentration = 5×10^{13} electrons/cm³. Mobility = 6×10^5 cm² V⁻¹ sec⁻¹. Applied electric field: 23.8 V/cm. $B = 5$ K Gauss.

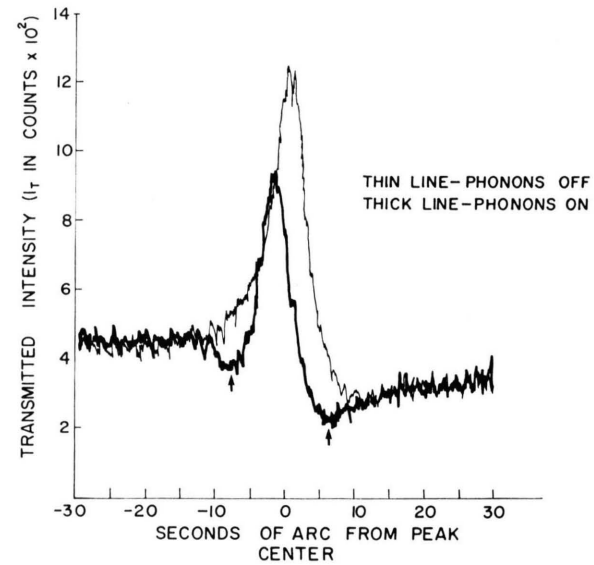


Fig. 6. Experimental results for the (004) thin crystal Laue transmission forward diffracted beam. The crystal is tilted around the diffraction vector so that the [110] axis forms an angle of 60° with the diffraction plane. Carrier concentration: 8×10^{13} electrons/cm³. Mobility: 7.0×10^5 cm² V⁻¹ sec⁻¹. Applied electric field: 10.3 V/cm. $B = 3.0$ K Gauss. Thickness: 0.312 mm. $\mu_0 t_{eff} \approx 3.8$.

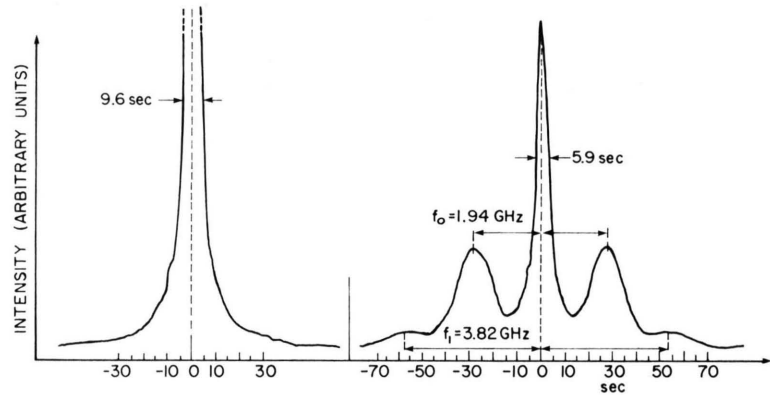


Fig. 5. Same as Fig. 4 except: carrier concentration: 3.5×10^{14} electrons/cm³. Mobility: 5×10^5 cm² V⁻¹ sec⁻¹.

3. Multiple Diffraction Effects from Non-Equilibrium Phonons

One of the interesting problems still open in diffraction physics is the mechanism of interaction between x-ray photons and phonons. For a thermal distribution of phonons it has been shown theoretically [9] and experimentally [10] that the same dynamical theory for a non-vibrating crystal holds, provided the scattering factors involved f_{hkl} are multiplied by their own Debye-Waller factors e^{-M} . This is obtained in a situation in which the phonons are totally incoherent, randomly polarized, of relatively weak intensity, and span a continuous and broad range of wave vectors, both in magnitude and direction. It is not clear that the same rule applies to highly coherent, intense and monochromatic phonon beams. A convenient technique for studying this problem makes use of the Acousto-Electric (A.E.) effect, for amplifying thermal phonons of selected modes and frequencies [11]. A piezoelectric crystal (in our case, InSb, which can be grown almost dislocations-free) is cut in the form of a long and thin bar, typically parallel to [110], and an electric field of a few tens of volts/cm is established parallel to [110]. Under suitable conditions, an intense phonon beam is generated with \mathbf{q} vector parallel to [110] and polarized along 001. (This is called "Fast Transverse [110] Acoustic Mode", or briefly: FT [110].) The frequency of the phonons is determined by the carrier concentration, temperature and other parameters [11]. Since the A.E. phonons are almost monochromatic, satellite reflections are generated at positions $\mathbf{G} \pm l\mathbf{q}$, where \mathbf{G} is any reciprocal lattice vector, l is any integer, positive or negative, and \mathbf{q} is the phonon wave vector. Since the ratio q/G is typically of the order of 10^{-4} , the satellite reflections are very close to the Bragg reflections, and high resolution is needed in order to see these satellites. Preliminary results in reflection (Bragg case) and in transmission (Laue case) have been published a few years ago (Refs. [12] and [13] respectively). Figures 4 and 5 show two Bragg diffraction profiles for two different frequencies. It is clear, particularly in Fig. 4, that there are wide angular ranges in which both satellites and Bragg peak are simultaneously excited. It is also clear that the satellite peak intensities are comparable to that of the Bragg peak, which makes kinematic theory, upon which the standard theory of Thermal Diffuse Scattering is based [14], unap-

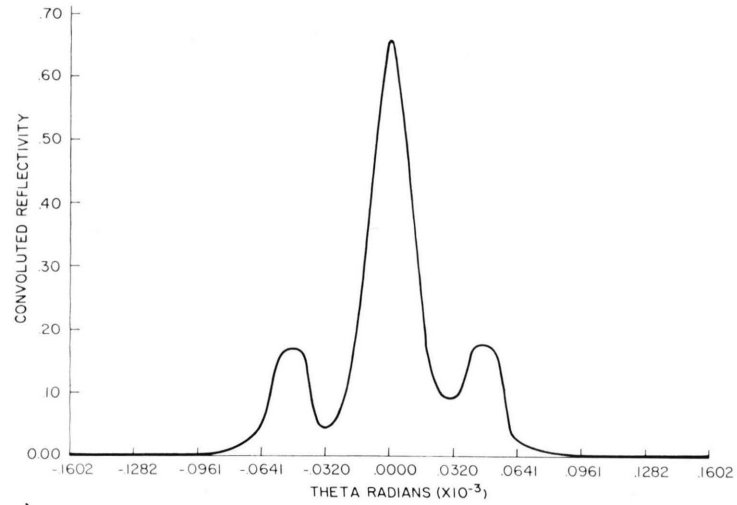
plicable to this case. Figure 6 shows an experiment with the Laue transmission geometry, in the thin crystal region ($\mu t \cong 3.8$). In this case two "dips", marked by arrows in the figure, are observed at θ values at which satellites would be observed in the Bragg case. A diffraction theory applicable to these experiments must necessarily be a dynamical theory. Such a theory has been developed by Koehler, Möhling and Peibst [15]. In this theory phonons are introduced at the outset. For a single phonon the following set of equations is obtained:

$$(k_0^2 - \beta_{il}^2) \mathbf{D}_{il} - \sum_{jp} \psi_{i-j} J_{l-p} (2\mathbf{G}_{i-j} \cdot \mathbf{U}) \cdot [(\boldsymbol{\beta}_{il} \cdot \mathbf{D}_{jp}) \boldsymbol{\beta}_{il} - \beta_{il}^2 \mathbf{D}_{jp}] = 0 \quad (3.1)$$

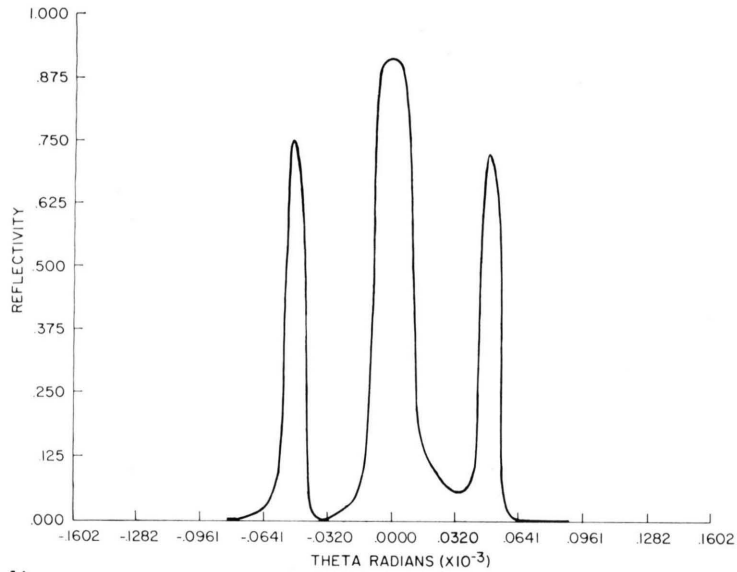
which is very similar to the standard dynamical equations (2.1) except for the fact that each (3.1) is associated with two indices instead of one, i and l , which identify a particular node in reciprocal space and the order number of a given satellite, respectively.

J_{l-p} are the Bessel functions of integer order and \mathbf{U} is the lattice displacement amplitude of the phonon. The system of Eqs. (3.1) can be solved using the same procedure outlined in Sect. 2 in order to calculate diffraction profiles. Our computer program has been modified accordingly, and some of the results are described below. The amplitude of the phonon waves is introduced as a parameter in the argument of the Bessel functions. Figures 7 and 8 show two calculated profiles, for low and high frequency phonons, respectively. Only first order satellites are introduced in the calculations. It is clear that the basic features of the experimental profiles are correctly reproduced. Note, in Fig. 7, the asymmetry between left and right satellites, also visible in the experiment (Figure 4). This asymmetry has to do with the different values of dynamical absorption operating on the wings of the Bragg peak, which are associated with different wave fields. Figure 9 shows the effect of introducing in the calculations second order satellites, which are visible in many of the experimental profiles.

Our computer program can also be used to calculate diffracted intensities in the Laue case, after minor modifications. Once the boundary conditions are solved, the intensities of all the vacuum waves can be calculated. An example is given in Fig. 10, in which wiggles are observed in correspondence of the "dips" observed in the experiment (Figure 6).



a)



b)

Fig. 7. Diffraction profiles with satellites due to acousto-electric phonons, calculated using n-beam dynamical theory. InSb(004). Wavelength of x-rays: $\lambda = 0.709 \text{ \AA}$. Frequency of phonons: $\nu = 0.69 \text{ GHz}$. Amplitude: $U = 0.065 \text{ \AA}$. Part a): convoluted with profile

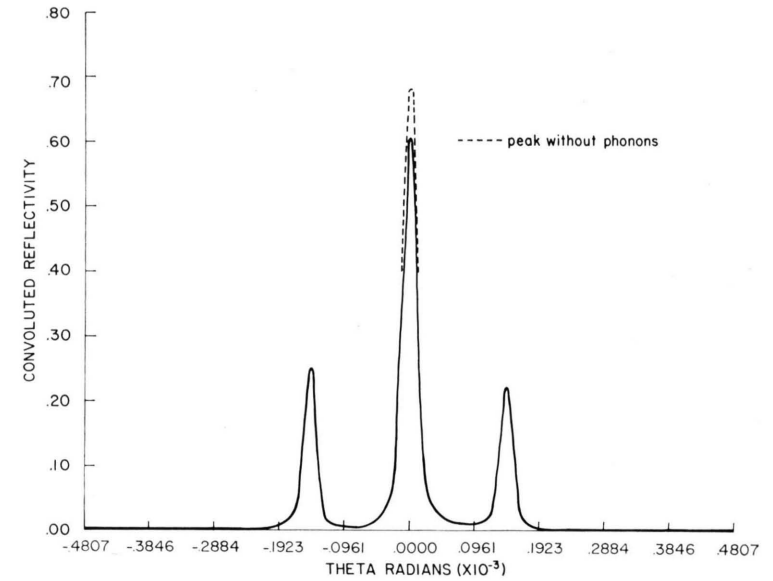


Fig. 8. Same as Fig. 7 except for: $\nu = 2.1 \text{ GHz}$. $U = 0.10 \text{ \AA}$.

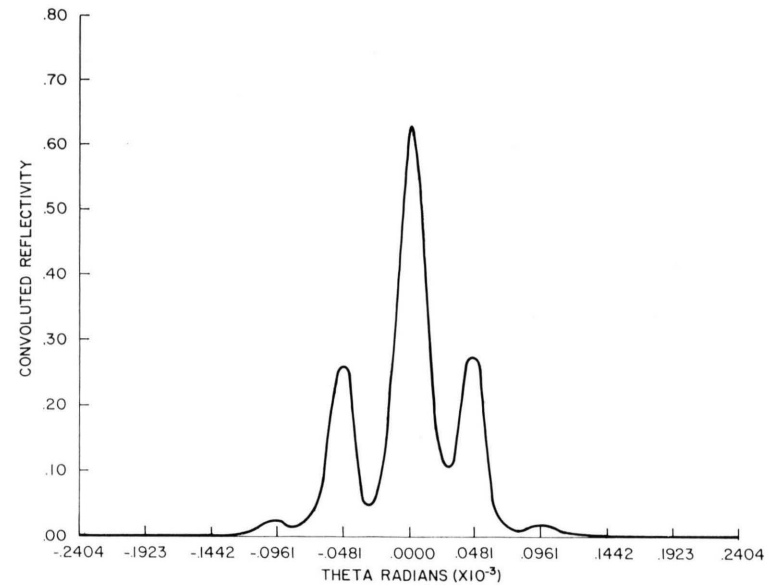


Fig. 9. Same as Fig. 7 except for: $\nu = 0.69 \text{ GHz}$, $U = 0.10 \text{ \AA}$. Two-photon processes are introduced in the calculations. Second order

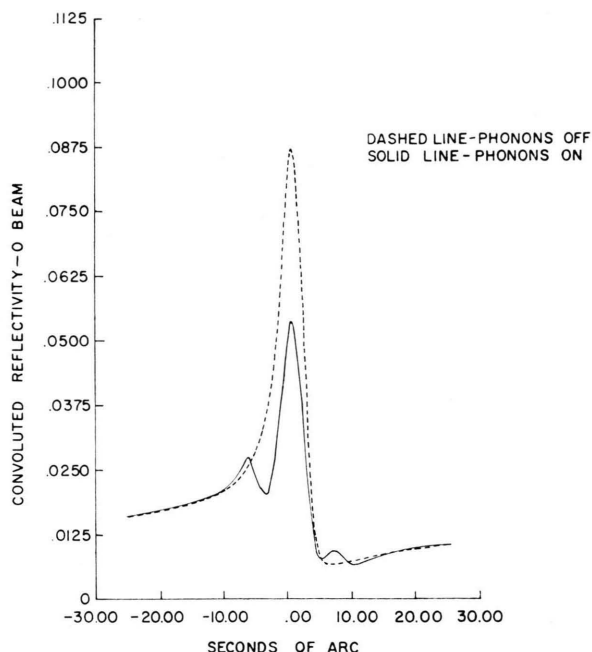


Fig. 10. Calculated forward diffracted beam for (004) thin crystal Laue transmission with a 60° tilt angle between the [110] axis and the diffraction plane. Ag-K α radiation ($\lambda = 0.56 \text{ \AA}$). $\mu_0 t_{\text{eff}} \cong 4.0$. Displacement amplitude: $U = 0.1 \text{ \AA}$. Frequency: $\nu = 0.67 \text{ GHz}$.

In essence, our n -beam dynamical theory, modified according to Koehler, Möhling and Peibst [15], explains all or most of the features observed in diffraction experiments in which strong phonon beams, amplified using the A.E. effect, are present.

There are, however, experiments in the Laue case in which the theory has failed. The reason for this failure is not clear at this time. It may have to do with the fact that inelastic scattering is not properly handled by the theory of [15]. More details will be given in a paper in preparation [16].

4. "Virtual Bragg Scattering" and the Phase Problem

Any time a given (hkl) structure factor is measured with great accuracy using the symmetric Bragg case [17], care is taken to avoid exciting simultaneous reflections by rotating the crystal around the scattering vector and making sure that the intensity does not depend on the azimuth φ . When the (hkl) reflection is weak (a typical case in point is the (222) in silicon and germanium) there

are many peaks in the Renninger plot [4] and the rule of the thumb is that φ must be chosen to be in the middle of a range $\Delta\varphi$, free of Umweganregung peaks, of at least $3-4$ degrees. Since the divergence of the incident beam perpendicular to the diffraction plane is typically $0.5-1^\circ$, the criterion of choosing a region $\Delta\varphi/2 \cong 1.5-2^\circ$ is taken to be a sufficient guarantee that multiple diffraction effects are absent. This consideration is corroborated by plots of the kind shown in Fig. 1, which demonstrates that the half width of a typical Umweganregung peak, on the φ -scale, is of the order of $20-30$ seconds of arc. The assumption is made that the ordinate value R^θ in Fig. 1 will reach quickly the asymptotic value corresponding to the "true" (222), more or less in the same way as the reflected intensity in a typical 2-beam rocking curve vanishes on the tails of the diffraction profile.

Interestingly enough, it has been found in the course of some experiments in our laboratory that this is not the case. It has been found that the (222) of silicon, when measured with a long wavelength (Cr-K α ; $\lambda = 2.29 \text{ \AA}$), which provides large umweg-free regions, is affected by multiple diffraction even at angles $\varphi - \varphi_0$ of the order of 4° , where φ_0 is the azimuth of an Umweganregung peak. Our beam had a divergence in the plane perpendicular to the diffraction plane of the order of 0.7° , as evidenced by the width $\Delta\varphi$ of the Umweganregung peaks, measured at half peak intensity. It appears that n -beam excitation falls off with the azimuthal angle φ much more slowly than ordinary 2-beam excitation does with the angle of incidence θ . This consideration is corroborated by evaluating the distances of the reciprocal lattice nodes involved from the Ewald sphere. It is calculated that, for a recovery of the asymptotic value of the intensity within 5% (which is zero in the 2-beam case), the extra nodes responsible for n -beam excitation (in our experiment: the $1\bar{1}1$ and $1\bar{1}\bar{1}$) have distances of the order of 2% of the radius, whereas in a typical 2-beam situation the same degree of excitation would be found at 0.001% of the radius. It is clear that a new mechanism is operating in this case. We have called it "Virtual Bragg Scattering", because it involves Bragg reflections for which energy is not conserved, in analogy with similar transitions in nuclear and atomic physics. We would like to stress that, while the tails of an ordinary 2-beam diffraction profile can be interpreted by relaxing

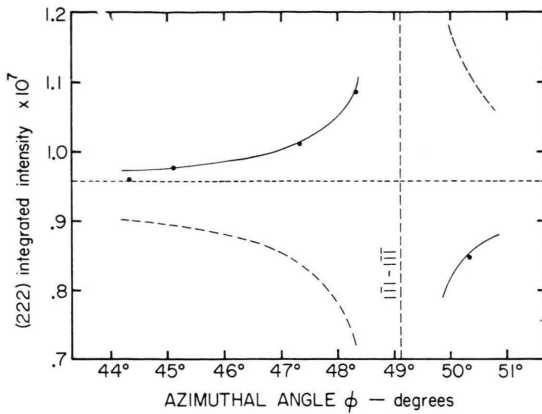


Fig. 11. Intensity of the (222) reflection as a function of azimuthal angle. Each point represents an integrated intensity with respect to θ , angle of incidence. Two strong Umweganregung peaks, with angles $3'$ apart, are located at a position marked by a vertical dotted line at $\varphi \cong 49^\circ 08'$. The two peak positions are not resolvable in this figure. Experimentally, one single peak is observed, 0.7° wide, with a peak intensity about a factor of 6.5 greater than the two-beam (222) value.

the condition of conservation of momentum parallel to the surface (and using Heisenberg's principle), the same is not applicable to the n -beam situation. Here momentum is always conserved, energy is not. The experimental data (see Figure 11), show the variation of a weak reflection in silicon (the (222)) as a function of the azimuthal angle φ in proximity of a strong Umweganregung peak due to two "extra" nodes ($1\bar{1}1$ and $1\bar{1}\bar{1}$) that are excited almost simultaneously. The calculations (solid line) are done using four beams. The agreement between theory and experiment is remarkably good. To see how sensitive are the results to the phases of the reflections involved, we arbitrarily changed the sign of one of the structure factors (the $1\bar{1}\bar{1}$) in the 4-beam calculations. In this case the dotted curve is obtained. The phase effect is unmistakable. We therefore prove in this way that the perturbations due to n -beam effects do contain phase information (as expected).

We also believe that this method can be applied to mosaic crystals, and that dynamical theory (the only one that preserves phase information) can be used to interpret the experimental results. The basis for this belief is the fact that the experimental intensity points plotted in Fig. 11 are all obtained in conditions of weak interaction between x-rays and crystal. In such a situation most scattering

events are single and dynamical and kinematic theory converge to the same result [18].

We therefore believe that making use of "Virtual Bragg Scattering" may lead to a solution of the phase problem in practical cases [19].

5. Multiple Diffraction Effects and Topography

In the course of some investigations of lattice defects produced by 2 Mev electrons in silicon using high resolution topography [20] some curious features were found in the pictures. The technique is essentially based on a double crystal geometry, both crystals being set for the Bragg case of diffraction. A conventional copper x-ray tube was used in all experiments, set in such a way that the point focal spot was utilized. The first crystal was highly asymmetric, set for grazing incidence, so that the diffracted beam was highly parallel in the diffraction plane. To achieve this condition, the first silicon crystal was cut parallel to the (577) planes within 1 minute of arc. The principle exploited in this technique is that the angle between the (577) and (511) planes is almost identical to the Bragg angle of Cu-K α_1 and Si-(511). The analytical formulae of 2-beam dynamical theory, such as those given in [7], are not applicable to this experiment, because they are derived under approximations that are not valid when the incident (or the diffracted) beam form very small angles with the surface. Using our computer program, in which no approximations are used, and setting $n = 2$, we calculate that the Bragg angle of K α_1 is $\theta_B = 4.04$ mrad, and that the width of the diffracted beam is about 0.1 sec, whereas the width of the incident beam is 24 seconds. It is interesting to note that for such a crystal, rays undergoing the (511) Bragg reflection are strongly optically reflected from the surface (32%) and that the overall penetration of the x-ray beam is limited to less than 1000 Å. The second crystal is a Si-(111) set for (333) diffraction (Bragg symmetric case). The beam leaving the first crystal has a cross section of 4–5 cm², so that a large area can be explored. The second crystal is carefully set on the side of the Bragg peak, in a region in which the intensity varies very rapidly with angle. In this way high sensitivity is obtained, because regions misoriented by less than 0.1 sec will reflect with different intensity [21]. The first crystal is absolutely perfect, and the assumption is made that only the second crystal

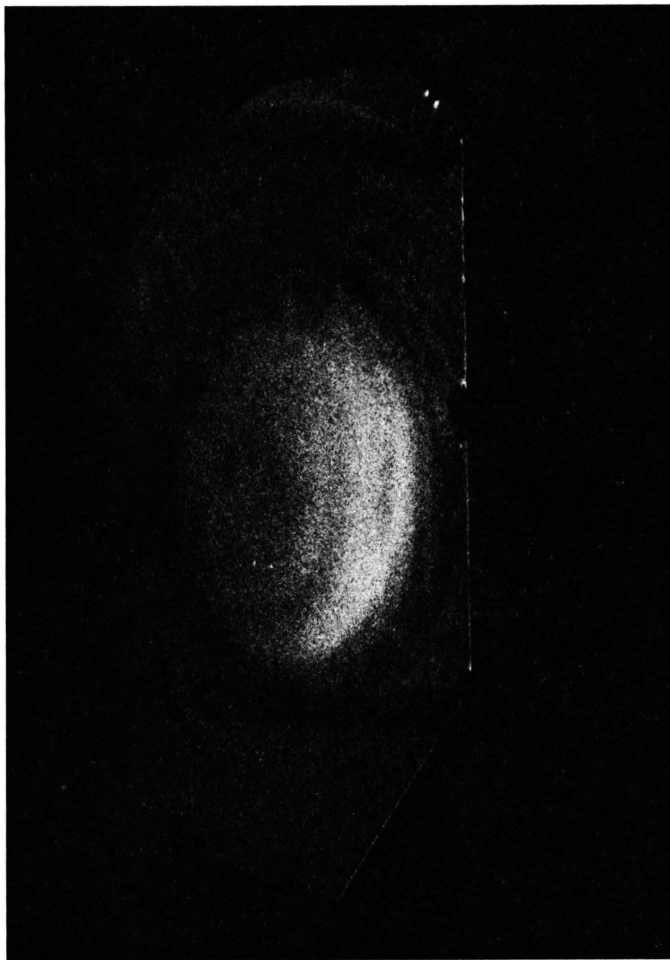


Fig. 12 Surface double crystal topograph of Si(333). The incident beam is highly collimated in the diffraction plane, and the sample crystal is set on the steep side of the reflection profile, at 65% reflectivity. The swirls visible in the picture correspond to regions of different lattice parameter ($\Delta d/d \cong 10^{-6}$). Note the two dark bands on top and bottom of the picture, due to 3-beam effects.

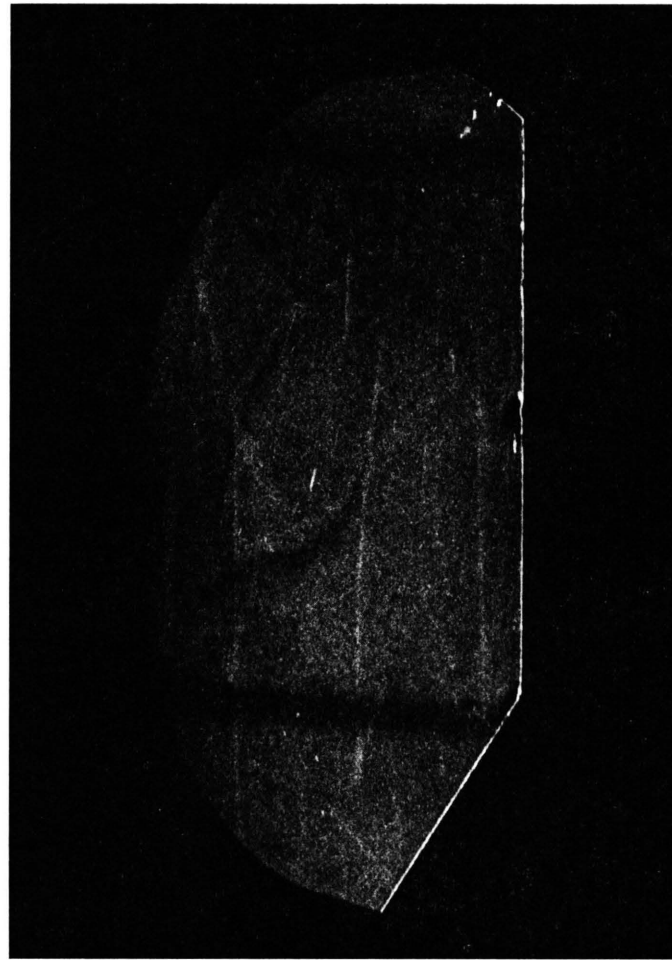


Fig. 13. Same as Fig. 12 except that the sample crystal is almost completely off the Bragg peak at 3% reflectivity. This is a kinematic region, and the beam penetrates deeper into the crystal. The swirls are no longer visible because the sensitivity to small changes in lattice parameter is lost but new features appear in the photograph. Again, note the two dark bands on top and bottom of the picture due to 3-beam effects.

may exhibit imperfections. Figures 12 and 13 show two examples of topographs obtained by this technique. We do not want to discuss the various features visible in these photographs. This is done elsewhere [20]. We want to concentrate our attention on the two dark bands running parallel on the top and bottom part of each photograph. It was noticed that *all* topographs, of very different crystals, had these dark bands. It was also found that the same dark bands would appear on films placed between first and second crystal. The presence of these bands seemed to be an intrinsic feature of the experimental technique independent of the particular choice of the first crystal, of the particular technique used for fastening the first crystal to its holder, etc.

It was conjectured that these bands might be due to multiple reflection effects.

It was verified that the width of the bands corresponds to the height of the focal spot, measured along a direction perpendicular to the diffraction plane. It would appear that for two particular values of the vertical [8] divergence angle φ the reflectivity of the (511) becomes close to zero. The first crystal is cut asymmetrically, therefore the azimuthal angle φ of the diffraction plane around the

diffraction vector is constant in all photographs. A closer examination of the geometrical conditions under which the first crystal is operating showed that the central part of Figs. 12 and 13 correspond to $\varphi_0 = 0.75\pi$, having chosen as reference ($\varphi = 0$) a $[01\bar{1}]$ direction lying on the diffraction plane, mostly antiparallel to the incident beam. It is found that close to φ_0 there are two values φ_1 and φ_2 . ($= \varphi_0 \pm 56$ minutes of arc) for which two other beams are excited, the $(11\bar{3}-202)$ and the $(1\bar{3}1-220)$, respectively. The distance between the two dark bands corresponds to these values of φ_1 and φ_2 . However, in order to really prove that the origin of the dark bands is due to 4-beam diffraction, a dynamical calculation should be done. We used the computer program based on the theory described in Sect. 2 and Ref. [6]. Since the theory is formulated in terms of an incident beam in the form of a plane wave, a series of $(511-1\bar{3}1-220)$ profiles have been computed for several values of φ centered on φ_2 . The profiles are shown in Figure 14. It is clear that in this case the excitation of two extra beams results in considerable attenuation of the main beam (Aufhellung). It is therefore demonstrated that the dark bands of Figs. 12 and 13 owe their origin to multiple beam effects.

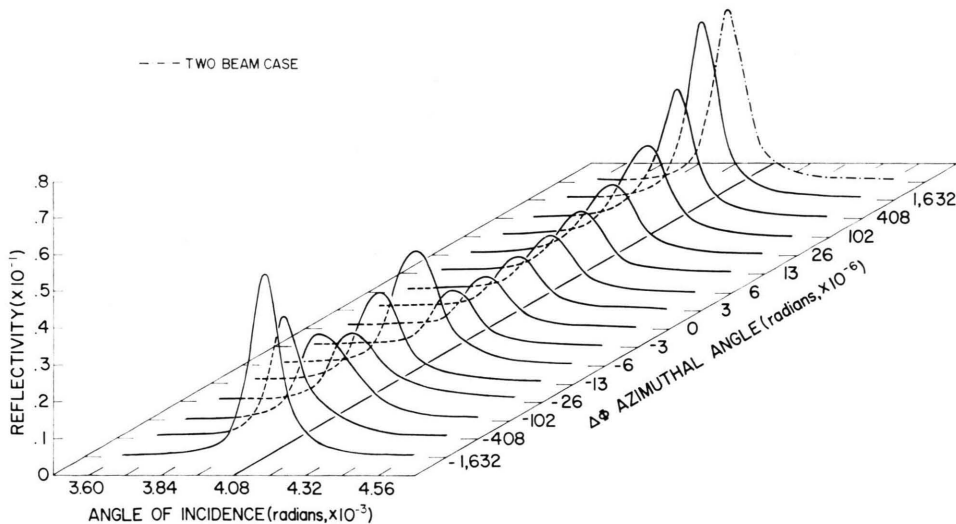


Fig. 14. Family of Si-(511) rocking curves as a function of the azimuthal angle φ around the diffraction vector. $\varphi = 0^\circ$ corresponds to the $[01\bar{1}]$ direction in the diffraction plane, mostly antiparallel to the incident beam. It is shown how the simultaneous excitation of the $(1\bar{3}1)$ and (220) reflections result in a strong reduction of the (511) diffracted intensity. $\Delta\varphi = \varphi - \varphi_{\min}$ where φ_{\min} is the azimuthal angle for which the peak reflectivity is minimum. The two-beam rocking curve is also shown for comparison.

6. Conclusions

N -beam diffraction is ordinarily considered a nuisance in structural crystallography because it introduces uncontrollable perturbations in measuring intensities. Conditions are therefore carefully chosen in order to avoid multiple reflections. We describe in this paper a number of situations in which n -beam diffraction has an interest in its own right, such as: i) the phase problem and the new concept of "Virtual Bragg Scattering"; ii) diffraction experiments in which intense non-equilibrium acoustic phonons are present in the crystal; iii) Bragg case diffraction topographs. A general method of solution is outlined and found to correctly interpret the experimental results in all cases.

7. Acknowledgements

The work described in this paper is the result of the author's collaboration with several people, without whom most of the work would not exist. The list includes former graduate students (S. D. Leroux, L. D. Chapman, R. D. Yoder) and my colleagues Professor R. Bray (for Sect. 2) and Professor A. Overhauser (for Sect. 4). Thanks are due to Professor R. Buschert and D. Kauffman at Goshen College who made available their unpublished results. Financial support from the National Science Foundation, Grant DMR-8108337 and the Materials Research Laboratory funded by the National Science Foundation, Grant DMR 80-20249, is gratefully acknowledged.

- [1] P. P. Ewald, *Ann. d. Physik* **49**, 117 (1916); **49**, 1 (1916); **54**, 519 (1917).
- [2] G. Borrmann and W. Hartwig, *Z. Krist.* **121**, 401 (1965).
- [3] G. Hildebrandt, *Phys. Stat. Sol.* **24**, 245 (1967).
- [4] A Renninger plot is a plot of R_{hkl} vs φ , where R_{hkl} is the intensity of a weak reflection, typically the 222 in diamond, silicon, or germanium, observed in the symmetric Bragg case, i.e., with the surface parallel to the (111) planes, as a function of φ , the azimuthal angle for rotations around the [111] direction.
- [5] The dash (') in front of the summation symbol indicates that the term with $i=j$ is omitted.
- [6] R. Colella, *Acta Cryst. A* **30**, 413 (1974).
- [7] W. H. Zachariasen, *Theory of X-Ray Diffraction in Crystals*, John Wiley, New York 1945.
- [8] "Vertical" means perpendicular to the diffraction plane.
- [9] Y. H. Ohtsuki, *J. Phys. Soc. Japan* **19**, 2285 (1964).
- [10] B. W. Batterman, *Phys. Rev.* **126**, 1461 (1962); **127**, 686 (1962); **134A**, 1354 (1964). B. Okkerse, *Philips Res. Repts.* **17**, 464 (1962).
- [11] See, for example, *Semiconductor Physics*, by K. Seeger, Sect. 7h; Springer Verlag, Berlin 1973.
- [12] S. D. Leroux, R. Colella, and R. Bray, *Phys. Rev. Letters* **35**, 230 (1975).
- [13] S. D. Leroux, R. Colella, and R. Bray, *Phys. Rev. Letters* **37**, 1056 (1976).
- [14] B. E. Warren, *X-Ray Diffraction*, Addison Wesley, 1969, Chapter 11.
- [15] R. Köhler, W. Möhling, and H. Peibst, *phys. stat. sol.* **41**, 75 (1970); **61**(b), 173 (1974).
- [16] D. L. Chapman, R. Colella, and R. Bray, in preparation.
- [17] This discussion does not need to be restricted to the symmetric Bragg case.
- [18] See, for example, discussion given for the Bragg case in a paper by P. H. Hirsch and G. N. Ramachandran, *Acta Cryst.* **3**, 187 (1950).
- [19] An ingenious technique for obtaining an extensive set of experimental data on n -beam interactions in perfect and mosaic crystals has been recently proposed by Jagodzinski (Ref. [22]), using a photographic method called "Noromosaic technique". The method is however qualitative, and does not lend itself to quantitative evaluations.
- [20] D. S. Kauffman, Ph. D. Thesis, in preparation (unpublished). Supervised by Prof. R. Buschert, Goshen College, Goshen, Indiana 46526.
- [21] U. Bonse, *Direct Observation of Imperfections in Crystals*, edited by J. B. Newkirk and J. W. Wernick, Interscience Publishers, 1962.
- [22] H. Jagodzinski, *Acta Cryst. A* **36**, 104 (1980).